Astronomical image reconstruction with deep convolutional neural networks

Rémi Flamary
Collaboration with : M. Moscu, R. Ammanouil, A. Ferrari, C. Richard

April 29, 2019, Séminaire Lagrange

Summary

Introduction

Supervised deep learning

Astronomical image reconstruction and inverse problem

Image reconstruction with deep learning

Network architecture

Training dataset

Numerical experiments

Constant Point Spread function

Varying Point Spread function

Conclusion

Introduction

Supervised learning

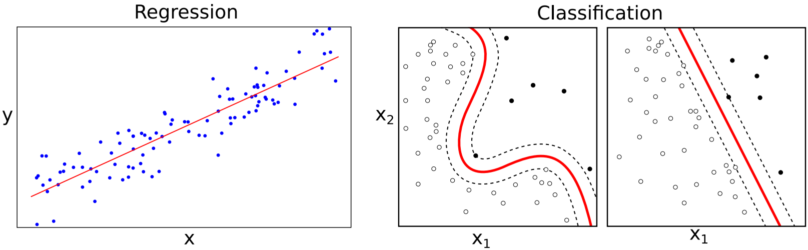

Supervised training of model $y = f(x)$

$$\min_f \sum_i L(y_i, f(x_i)) \tag{1}$$

- L is the prediction error.
- $\{y_i, x_i\}_i$ is the training dataset.
- What is f (linear, nonlinear, neural network) ?
- Model f should not be too complex (or overfitting).

Supervised deep learning

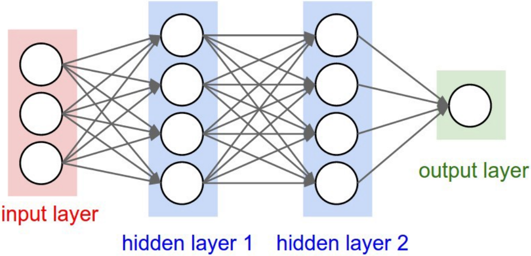

Deep neural network [LeCun et al., 2015]

$$f(x) = f_K(f_{K-1}(\ldots f_1(x)\ldots)) \tag{2}$$

- f is a composition of basis functions f_k of the form :

$$f_k(x) = g_k(W_k x + b_k) \tag{3}$$

- W_k is a linear operator and b_k is a bias for layer k.
- g_k is a non-linear activation function for layer k.
- Function f parameters : $\{W_k, b_k\}_k$.

Convolutional neural network

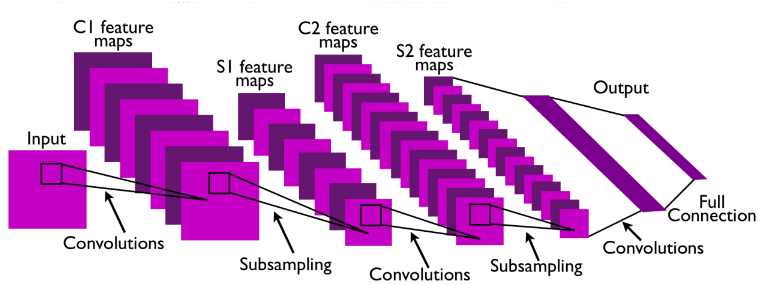

- Replace the linear operator by a convolution [LeCun et al., 2010].
- Reduce image dimensionality with sub-sampling or max pooling.
- Number of parameters depends on the size fo the filter, not the image.
- Recent deep CNN use Relu activation [Glorot et al., 2011] : $g(x) = \max(0, x)$

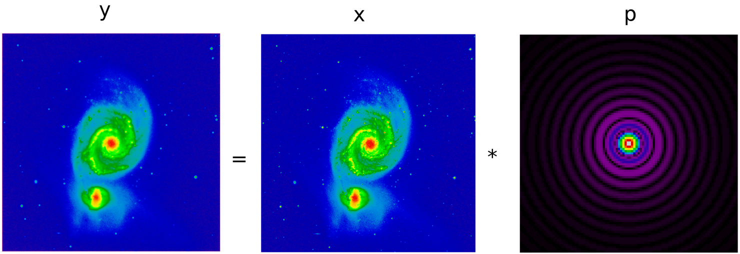

Astronomical image observation

- Convolutional model : $y = x * p$
  - y is the observed image (dirty).
  - x is the true image.
  - p is the Point Spread Function (PSF)
- Geometry of the telescope gives the Point Spread Function (PSF).
- Some noise due to the observation is also present (Gaussian,Poisson).
- On wide field of view the PSF can be space variant (Fredholm's integral).

Inverse problem

Image reconstruction

$$\min_{x} \quad L(y, x * p) \tag{4}$$

where L is a data fitting loss.

- We want to inverse the observation process.
- Reconstruct an estimation of the true image x from y.
- For every new observation one needs to solve the problem.
- Linear PSF interpolation for fast fft convolution [Denis et al., 2015].

Common approaches and algorithms

- Wiener filtering (inverse filtering+noise attenuation).
- [Richardson, 1972, Lucy, 1974], CLEAN [Högbom, 1974].
- Sparsity promoting regularization [Dabbech et al., 2015] [Deguignet et al., 2016].
- Iterative methods based on gradient (or proximal) descent.

Image reconstruction with deep learning

Training for image reconstruction

Deep learning for inverse problem [McCann et al., 2017]

- Train a function f that solves approximately the inverse problem.
- Move computational complexity to the training step.

Deep network for image reconstruction [Xu et al., 2014, Flamary, 2017]

$$\min_f \quad \frac{1}{2N}\sum_i^N \|x_i - f(y_i)\|^2$$

- f is the deep network with architecture tailored for image reconstruction.
- $\{x_i, y_i\}_{i=1\ldots N}$ are the clean/dirty image training dataset.
- Optimization of f is done once.
- Reconstruction for new image is $f(y)$.

Network architecture

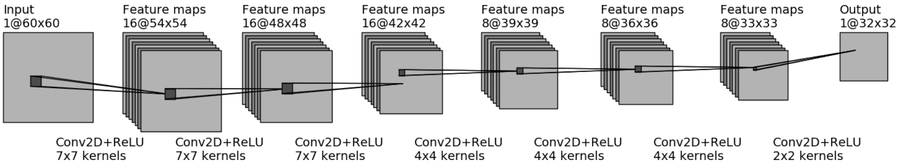

- Architecture is a classical 6 layers CNN.
- Each Layers consists in
  - a convolutional layer with small 2D filters,
  - a Relu activation of the form $g(x) = \max(0, x)$ [Glorot et al., 2011] .
- Exact convolution leads to an output smaller than the input (60→32).
- The network is stationary and can be adapted to any image size.
- Reconstruction can be done on patches or one large image.
- Relu is good for deep learning because it has no vanishing gradients.

Training dataset

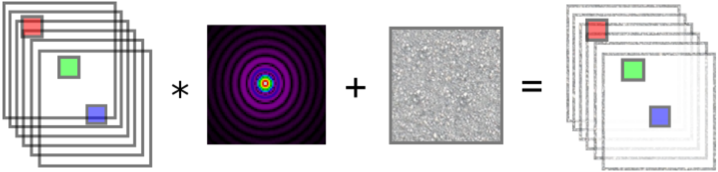

- Dataset is generated online from true/observed images.
- We randomly draw patches from training images and add random noise.
- Generated noise ensure that a sample is never seen twice by the network.
- We use 6 large images of size 3564x3564 from STScIDigitized Sky Survey, HST Phase 2 dataset.
- Performance is evaluated with One-VS-All approach (train on 5 images, test on the 6th).

Training dataset

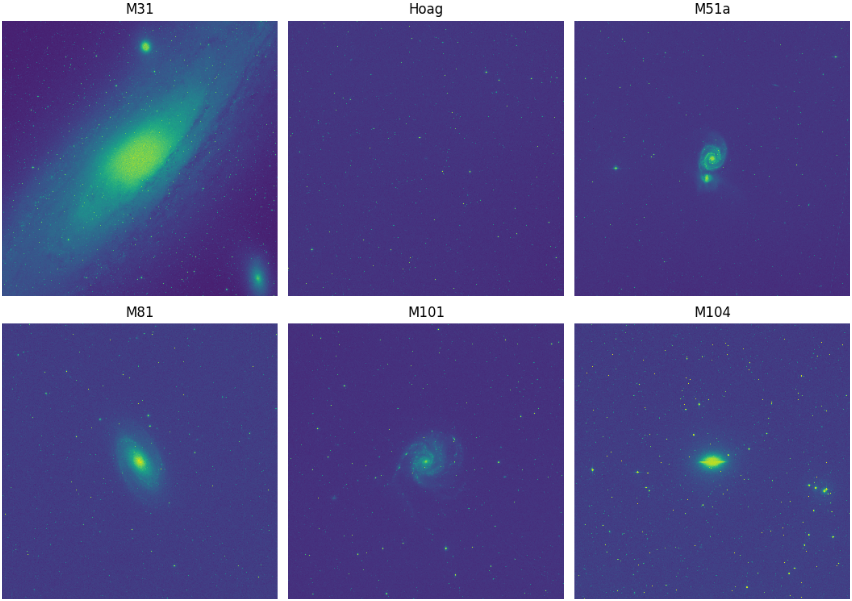

Training dataset

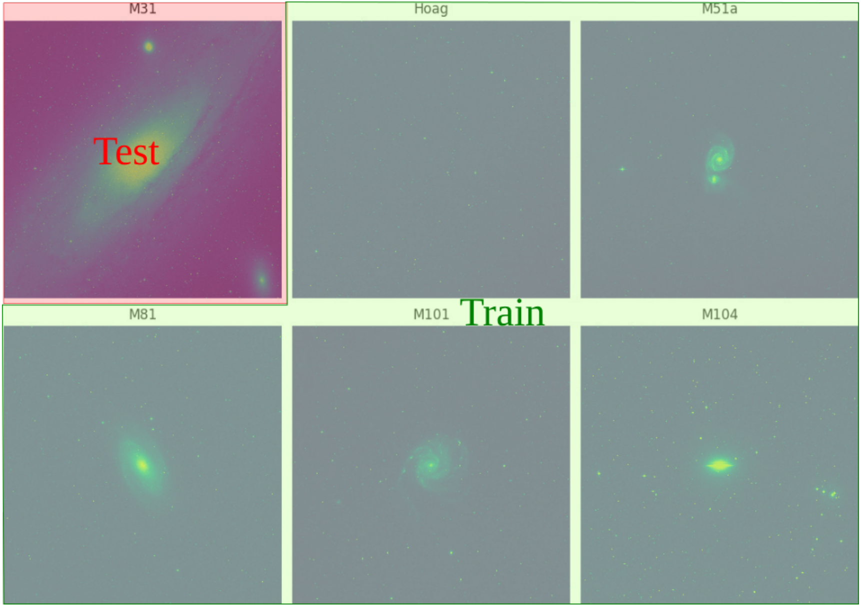

Numerical experiments

Constant PSF : data and protocol

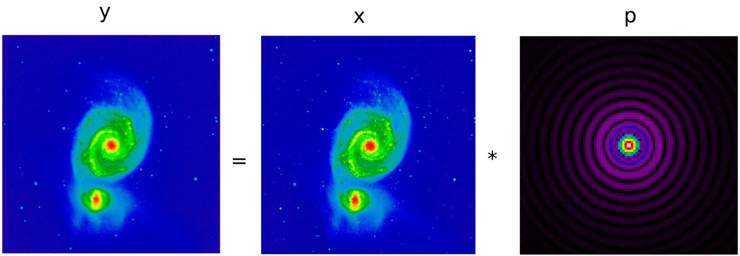

- We use the central 1024x1024 pixels images for comparison.
- Data normalized to a maximum value of 1.
- PSF for a circular apperture : $p(r) = I_0(J_1(r)/r)^2$
- Radius of PSF r scaled so that we have 100 rebounds in the image.
- Gaussian noise of standard deviation $\sigma = 0.01$.

Constant PSF : numerical performances

Image \ Method	Wiener	RL	Prox	DCNN	CNN0
M31 : 31.83	31.88	31.17	**31.98**	31.26	31.44
Hoag : 35.39	36.70	36.77	36.76	**40.04**	37.98
M51a : 35.81	37.29	37.16	38.39	**39.89**	38.16
M81 : 34.23	35.05	34.82	35.91	**36.79**	36.02
M101 : 34.71	35.97	36.28	36.63	**39.75**	37.78
M104 : 33.49	33.97	33.27	34.52	**35.39**	35.07
Avg. PSNR (dB)	35.14	34.91	35.70	**37.18**	36.11
Avg. time (s)	**0.22**	4.94	593.42	1.65	0.44

- DCNN has best PSNR on all images except M31.
- Importance of representative dataset.
- Prox works best of all other methods but important numerical cost.
- 1024*x*1024 image reconstructed in 1.65 seconds.

Constant PSF : Visual comparison

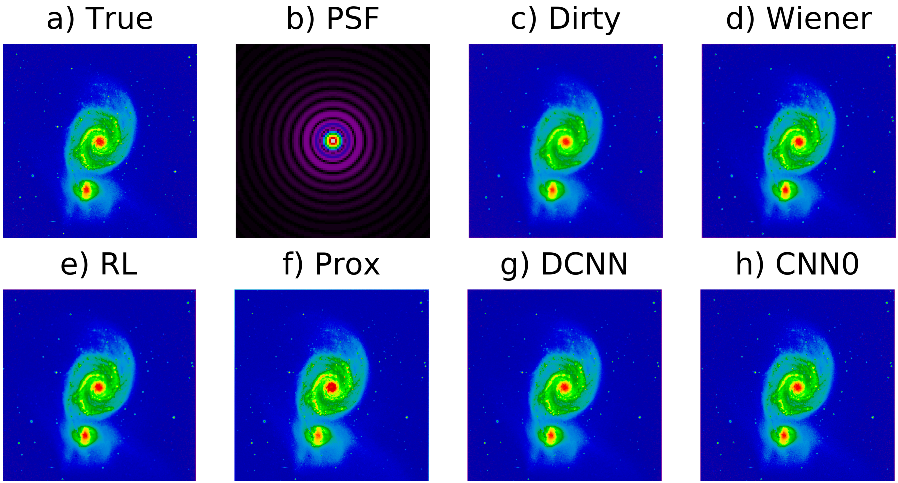

- Visual comparison for different methods.
- PSF is zoomed and represented with its square root.

Constant PSF : Model Interpretation

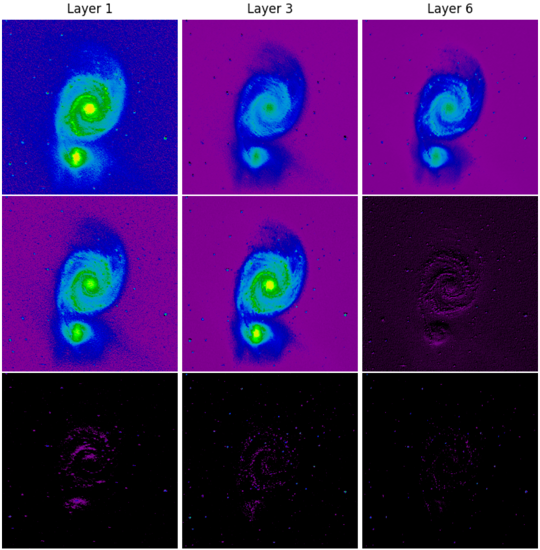

Varying PSF : data

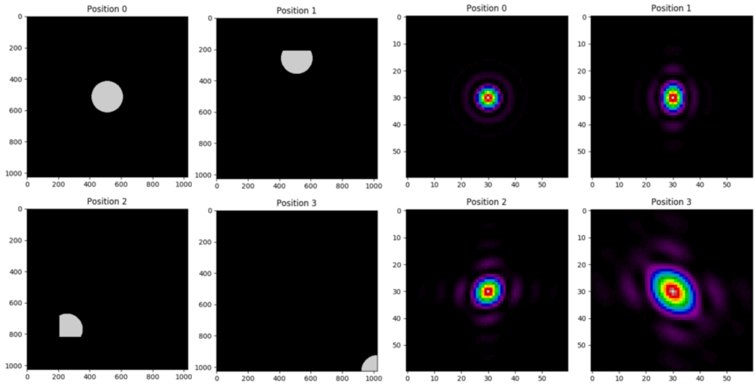

- PSF for circular aperture at the center of the image.
- Varying PSF corresponding to box occultation in a wide field.
- Pre-compute exact Fredholm's integral on the images.

Varying PSF : data

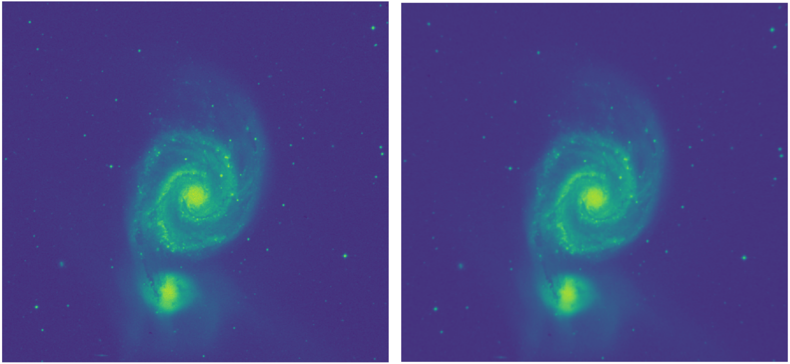

- PSF for circular aperture at the center of the image.
- Varying PSF corresponding to box occultation in a wide field.
- Pre-compute exact Fredholm's integral on the images.

Varying PSF : numerical performances

Image \ Method	Wiener	RL	RL SV9	Prox	Prox SV3	Prox SV5	DCNN C	DCNN SV
M31 : 18.60	18.61	18.45	18.59	18.74	18.74	18.75	18.28	**23.40**
Hoag : 32.66	33.37	32.61	32.91	33.62	33.58	33.62	32.26	**40.45**
M51a : 29.32	29.52	29.43	29.43	29.75	29.75	29.76	29.03	**39.02**
M81 : 33.50	34.42	33.27	33.79	34.42	34.38	34.44	32.83	**35.82**
M101 : 32.52	33.21	32.46	32.71	33.48	33.46	33.50	31.91	**39.35**
M104 : 32.30	33.01	31.38	32.45	33.16	33.12	33.17	31.16	**35.15**
Avg. PSNR (dB)	30.35	29.60	29.98	30.53	30.50	30.54	29.25	**35.53**
Avg. time (s)	**0.36**	1.41	133.20	1510.87	11381.24	24054.04	1.64	1.60

- Best PSNR for DCNN methods, same complexity as constant PSF.
- Only slight advantage to the PSF interpolation because of limited sampling.
- DCNN SV learn to simultaneously estimate the PSF and reconstruct a patch.
- Other kind of invariance can be incoded in dataset (misalignement,wavefront,...).

Varying PSF : Visual comparison

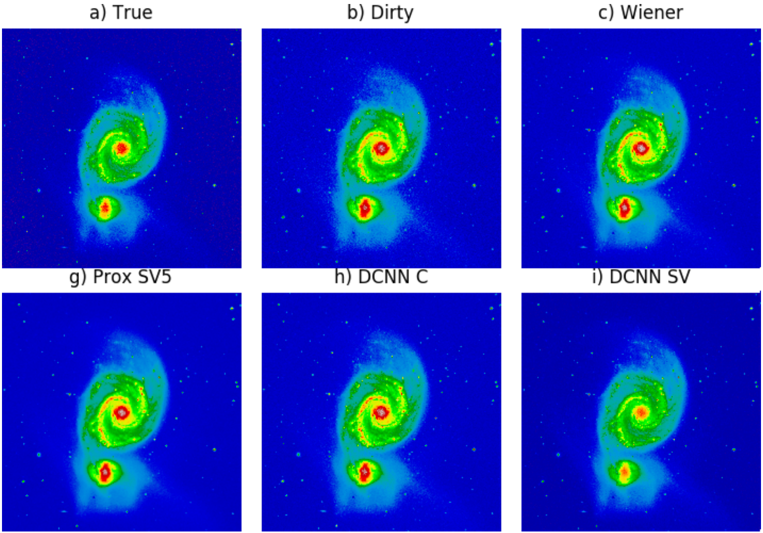

Varying PSF : Model Interpretation

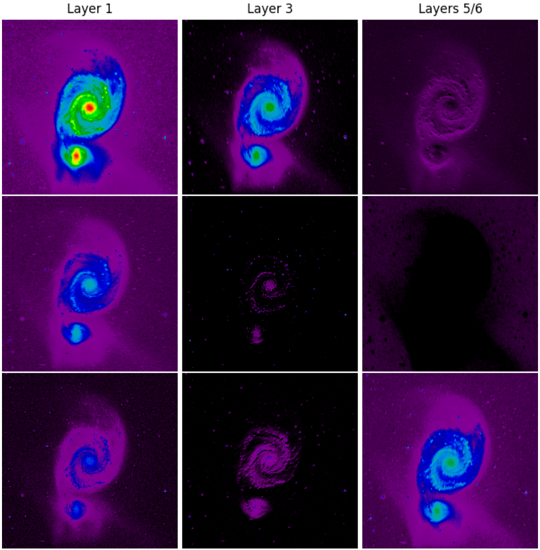

Conclusion

Conclusion

Astronomical image reconstruction with DCNN [Flamary, 2017]

- Relatively low processing time.
- Linear complexity w.r.t. number of pixels.
- Filter interpretability.
- One-time solving of an optimization problem.
- Robustness to different PSF (if learned).

What next ?

- Residual nets for a more multiscale reconstruction.
- Fast image reconstruction for adaptive optics.
- Reconstructing hyperspectral images.

Numerical comparisons

Constant PSF

- Wiener filtering with Laplacian regularization [Orieux et al., 2010].
- Richardson Lucy [Richardson, 1972, Lucy, 1974].
- Proximal gradient descent with sparse wavelet regularization and automatic regularization estimation [Ammanouil et al., 2017].
- Shallow CNN with 1 linear Layer, supervised Wiener (CNN0).
- Proposed Deep CNN (DCNN).

Space variant PSF

- Approximate variation with linear interpolation [Denis et al., 2015].
- Adaptation of Richardson-Lucy and Proximal gradient descent using FFT.
- Comparison of DCNN learned on fixed center PSF (DCNN C) and on variant PSF (DCNN SV).

Model estimation

Estimation problem

$$\min_{f} \quad \frac{1}{2N} \sum_{i}^{N} \|x_i - f(y_i)\|^2$$

- The full model has $\approx$ 30000 parameters.
- Use a generator to draw randomly training samples.
- Optimization with stochastic gradient with minibatch.
- Two kind of minibatch for gradient computation :
  - Local due to the size of the patch.
  - Global due to the number of patch.
- Use Nesterov-type acceleration.
- Stop learning when the average loss do not decrease anymore.

Implementation

Python implementation

- Implementation using Theano/Keras.
- Train and predict using NVIDIA Titan X GPU.
- One epoch takes $\approx$ 45 seconds.

Training parameters (tricks of the trade)

- Parameter initialization with normalised Gaussian [Glorot and Bengio, 2010].
- Learning rate=0.01, momentum=0.9.
- Minibatch of size 50 patches.
- Epochs of 300 000 samples.
- Restart initialization if no change in loss after one epoch.

Varying PSF : fast PSF Interpolation

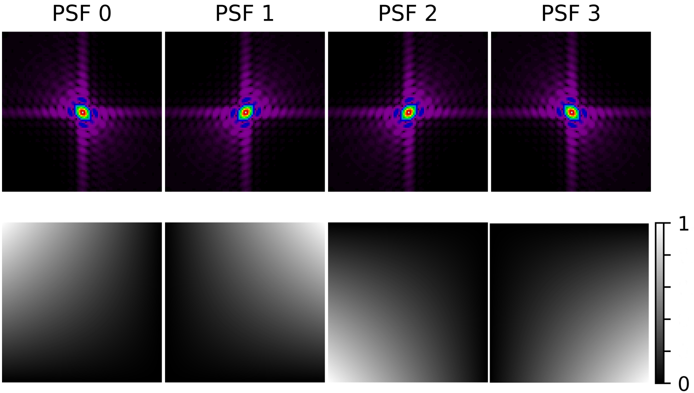

$$z_{conv} = \sum_{m=0}^{M-1} \omega_m \odot (x * p_m) \tag{5}$$

-
- Bilinear PSF interpolation for a simple 2 by 2 grid.
- FFT can still be used for fast convolution of each base PSF.

References

References i

Ammanouil, R., Ferrari, A., Flamary, R., Ferrari, C., and Mary, D. (2017). **Multi-frequency image reconstruction for radio-interferometry with self-tuned regularization parameters.** *CoRR*, abs/1703.03608.

Dabbech, A., Ferrari, C., Mary, D., Slezak, E., Smirnov, O., and Kenyon, J. S. (2015). **Moresane : Model reconstruction by synthesis-analysis estimators-a sparse deconvolution algorithm for radio interferometric imaging.** *Astronomy & Astrophysics*, 576 :A7.

Deguignet, J., Ferrari, A., Mary, D., and Ferrari, C. (2016). **Distributed multi-frequency image reconstruction for radio-interferometry.** In *Signal Processing Conference (EUSIPCO), 2016 24th European*, pages 1483–1487. IEEE.

Denis, L., Thiébaut, É., Soulez, F., Becker, J.-M., and Mourya, R. (2015). **Fast Approximations of Shift-Variant Blur.** *International Journal of Computer Vision*, 115(3) :pp 253–278.

Flamary, R. (2017). **Astronomical image reconstruction with convolutional neural networks.**

Glorot, X. and Bengio, Y. (2010). **Understanding the difficulty of training deep feedforward neural networks.** In *Proceedings of the Thirteenth International Conference on Artificial Intelligence and Statistics*, pages 249–256.

Glorot, X., Bordes, A., and Bengio, Y. (2011). **Deep sparse rectifier neural networks.** In *Aistats*, volume 15, page 275.

Högbom, J. A. (1974). **Aperture Synthesis with a Non-Regular Distribution of Interferometer Baselines.** *Astronomy and Astrophysics Supplement*, 15 :417.

LeCun, Y., Bengio, Y., and Hinton, G. (2015). **Deep learning.** *Nature*, 521(7553) :436–444.

LeCun, Y., Kavukcuoglu, K., and Farabet, C. (2010). ***Convolutional networks and applications in vision*, pages 253–256.**

Lucy, L. B. (1974). **An iterative technique for the rectification of observed distributions.** *The astronomical journal*, 79 :745.

McCann, M. T., Jin, K. H., and Unser, M. (2017). **A review of convolutional neural networks for inverse problems in imaging.** *arXiv preprint arXiv :1710.04011*.

Orieux, F., Giovannelli, J.-F., and Rodet, T. (2010). **Bayesian estimation of regularization and point spread function parameters for wiener–hunt deconvolution.** *JOSA A*, 27(7) :1593–1607.

Richardson, W. H. (1972). **Bayesian-based iterative method of image restoration∗.** *J. Opt. Soc. Am.*, 62(1) :55–59.

Xu, L., Ren, J. S., Liu, C., and Jia, J. (2014). **Deep convolutional neural network for image deconvolution.** In *Advances in Neural Information Processing Systems*, pages 1790–1798.